Lawrence Berkeley Laboratory
UNIVERSITY OF CALIFORNIA

Physics Division

Presented at the VIIth International Workshop on
Photon-Photon Collisions, Paris, France,
April 1-5, 1986

PHOTON-PHOTON PHYSICS WITH THE MARK II AT PEP

G. Gidal

April 1986

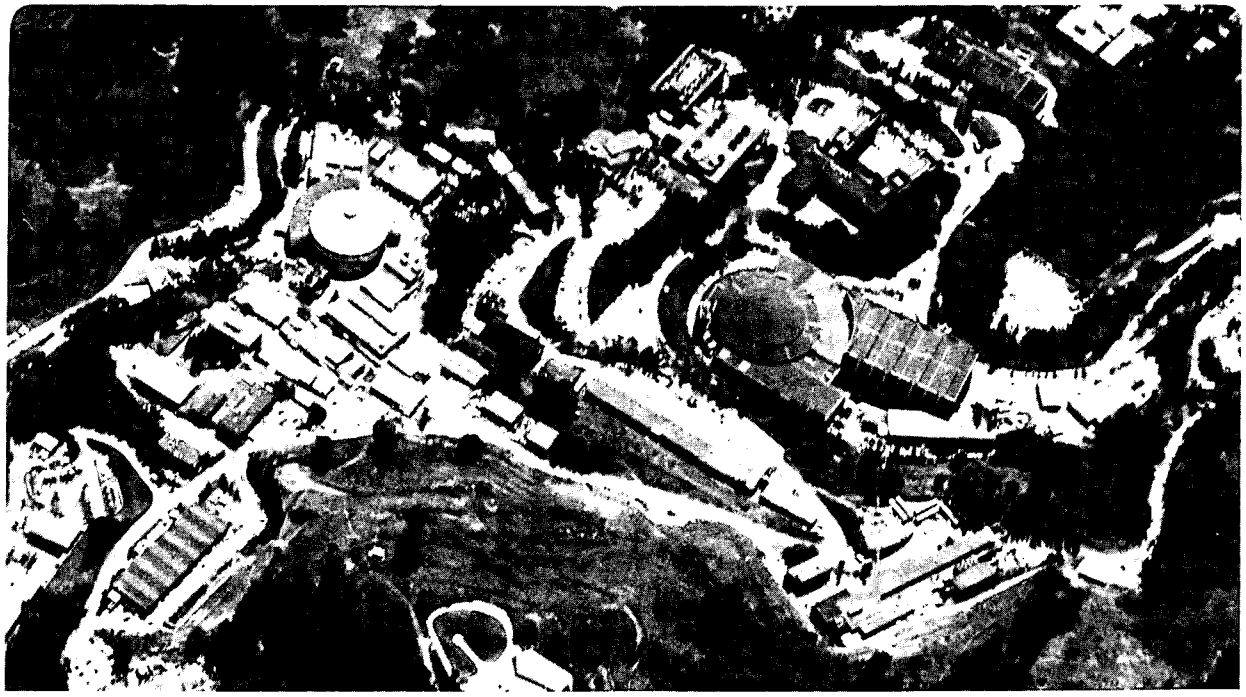

Prepared for the U.S. Department of Energy under Contract DE-AC03-76SF00098

DISCLAIMER

LBL-21818

Paper presented at the VIIth International Workshop on Photon-Photon Collisions, College de France, Paris, 1-5 April 1986

PHOTON-PHOTON PHYSICS WITH THE MARK II AT PEP*

G. Gidal

MARK II Collaboration

Lawrence Berkeley Laboratory and Department of Physics
University of California, Berkeley, California 94720

Stanford Linear Accelerator Center
Stanford University, Stanford, California 94305

Department of Physics
Harvard University, Cambridge, Massachusetts 02138

ABSTRACT

Photon-photon interactions are studied with the Mark II detector at PEP. The inclusive production of charged hadrons at large transverse momenta and the exclusive production of meson pairs at large invariant mass are compared with recent hard scattering calculations. Copious inclusive production of K^0's at large transverse momenta provides evidence for charm production. The radiative width of the f' (1520) is measured via its $K^0_S K^0_S$ decay mode.

We present results on inclusive hadron production in $\gamma\gamma^*$ interactions, high mass meson pair production, and the radiative width of the f' (1520), using the Mark II detector at PEP. The results are based on an integrated luminosity of 220 pb^{-1}. The major features of the Mark II detector have been well described elsewhere,[1] but as a reminder we show a schematic view in Fig. 1a.

*This work was supported in part by the Department of Energy under contracts DE-AC03-76SF00098, DE-AC03-76SF00515, and DE-AC02-76ER03064.

Fig. 1a

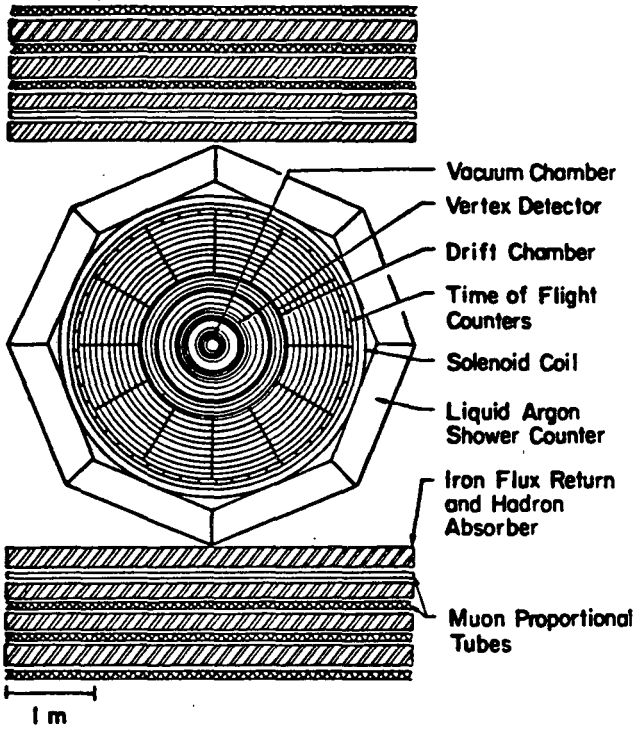

Fig. 1b

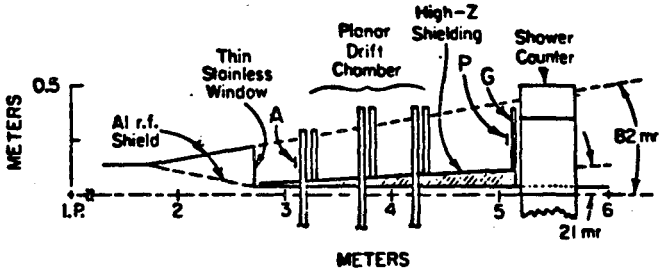

Fig. 2

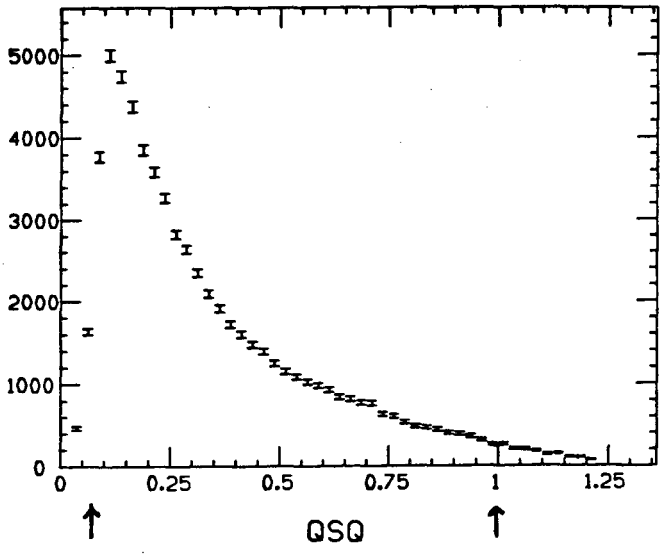

I. INCLUSIVE HADRON PRODUCTION IN $\gamma\gamma^*$ INTERACTIONS

The small angle tagging system, shown in Fig. 1b, measures electrons scattered between 21 and 83 mrads providing some 60,000 tagged events in the Q^2 interval between 0.075 and 1.00 GeV/c^2, distributed as in Fig. 2. Since we do not observe the entire final state, the transverse momentum of hadrons, p_T, is calculated in the usual manner, with respect to the e^+e^- beam axis. To eliminate the large QED background we accept only events with 3 or more charged prongs observed (in addition to the tagging electron). Identified leptons are removed using the Liquid Argon Calorimeter and the muon chambers. To minimize the beam-gas interaction background we also eliminate events with protons or deuterons identified by the time of flight. The background from $e^+e^- \rightarrow e^+e^-\tau^+\tau^-$ is subtracted using the Monte Carlo simulation of this process. The residual background from beam-gas interactions is simulated with events produced at larger z. Both these backgrounds vary between 5% and 10% with p_T and are subtracted. Taking advantage of the precision vertex chamber, the VFINDP program is used to find K^0's which decay at least 2.5 mm from the primary vertex. After several track quality cuts and three dimensional swimming of tracks to the secondary vertex, the $c\tau$ and $\pi^+\pi^-$ mass spectrum in Fig. 3 are obtained. The cuts shown then define the K^0 sample.

The GGDEPA (Vermasseren) Monte Carlo is used to simulate point like scattering, $e^+e^- \rightarrow e^+e^-q\bar{q}$, and the quarks are fragmented according to the LUND scheme.[2] This Monte Carlo is used to measure the efficiencies shown smoothed in Fig. 4. No Vector Dominance Model (VDM) Monte Carlo has yet been implemented. At large p_T we are still limited by Monte Carlo efficiency errors.

In Fig. 5 we then show the normalized $d\sigma/dp_T$ for $\gamma\gamma^* \rightarrow$ hadrons in the Q^2 range defined above. The steep fall off at low p_T is characteristic of VDM. The solid curve is based on a recent calculation of Aurenche et al.[3] for untagged $\gamma\gamma$ interactions. In this calculation, higher order QCD terms and generalized vector dominance model contributions (motivated by photoproduction data) were combined in an attempt to resolve the discrepancy between the Born term calculation and the untagged TASSO data.[4] The status of this comparison at last year's Kyoto conference is shown as a function of p_T^2 in Fig. 6. To compare this calculation to our own data, the Aurenche et al. curve is reduced by approximately 10 to compensate for the tagging interval used and the different value of $\sqrt{s}$. There are several sources of

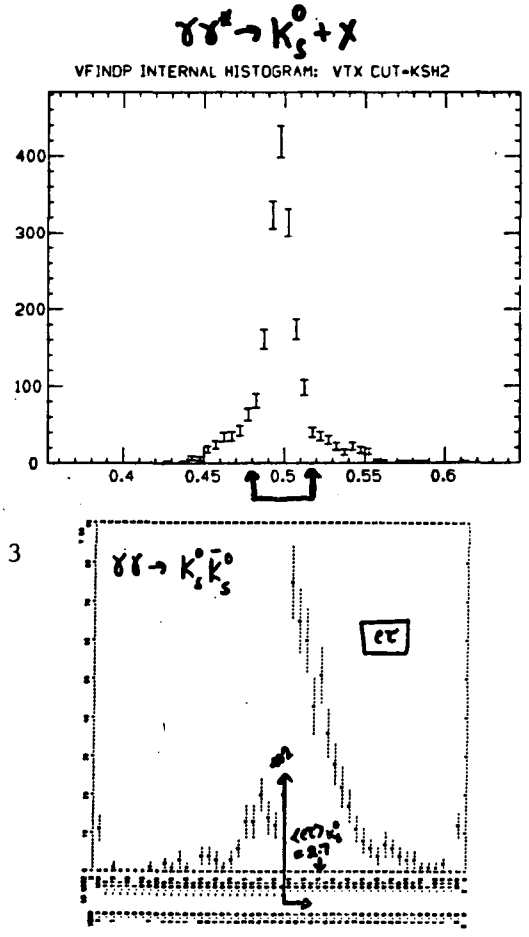

Fig. 3

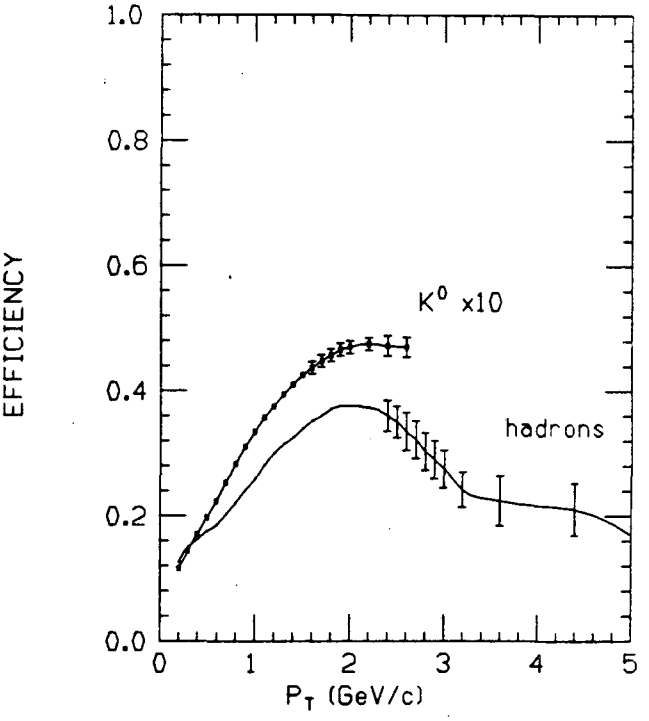

Fig. 4

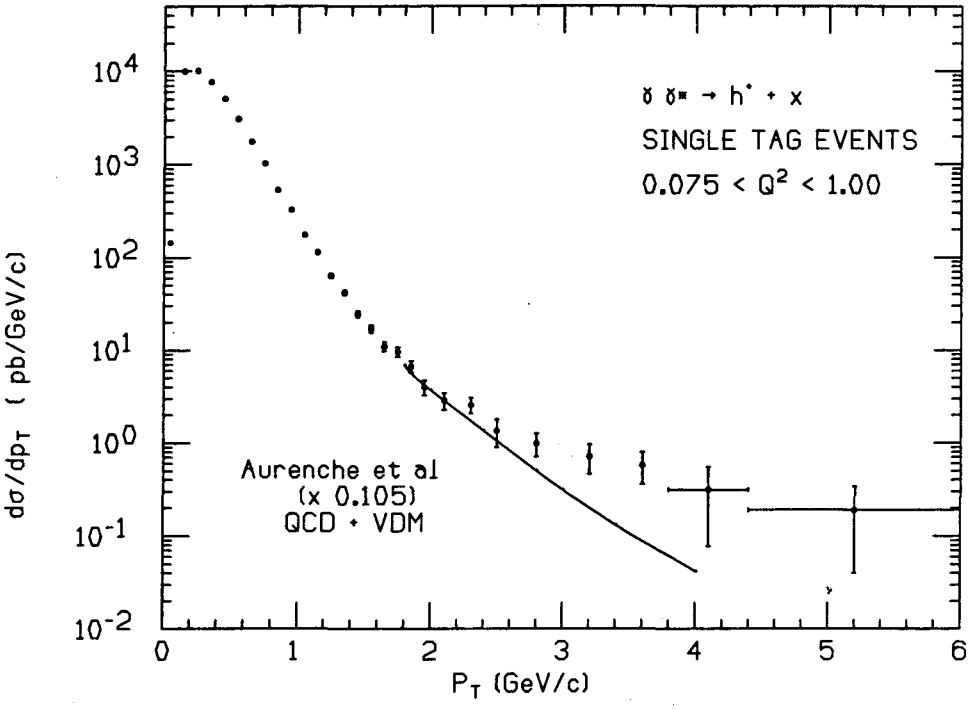

Fig. 5

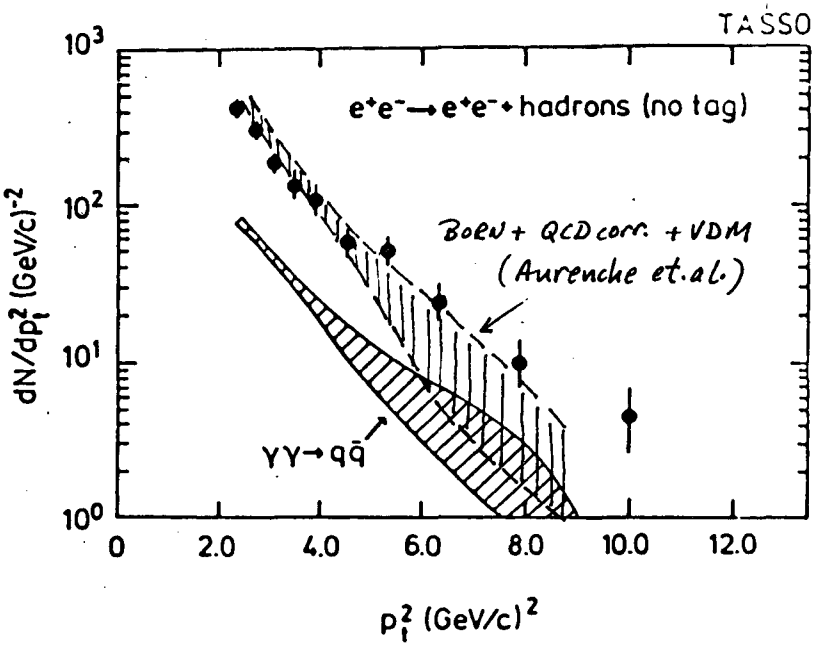

Fig. 6

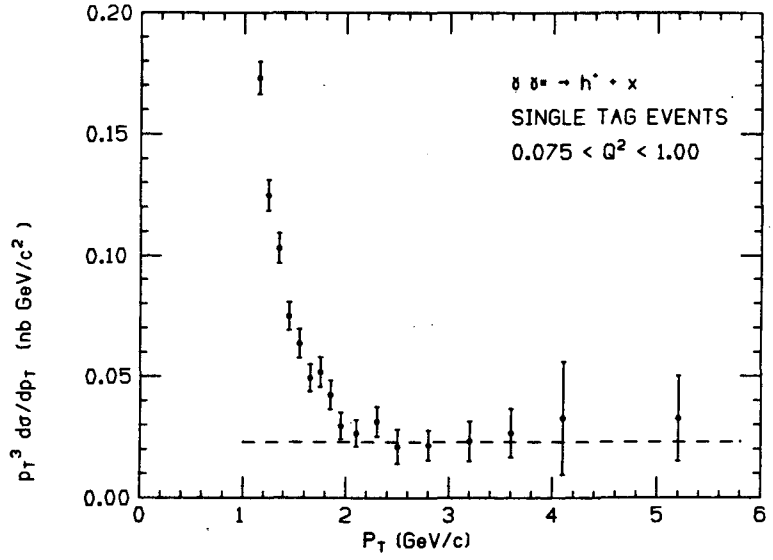

Fig. 7

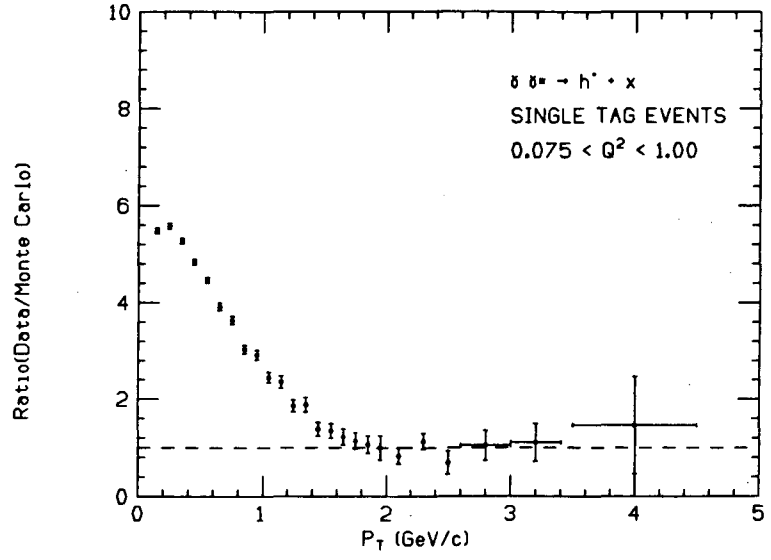

Fig. 8

Fig. 9

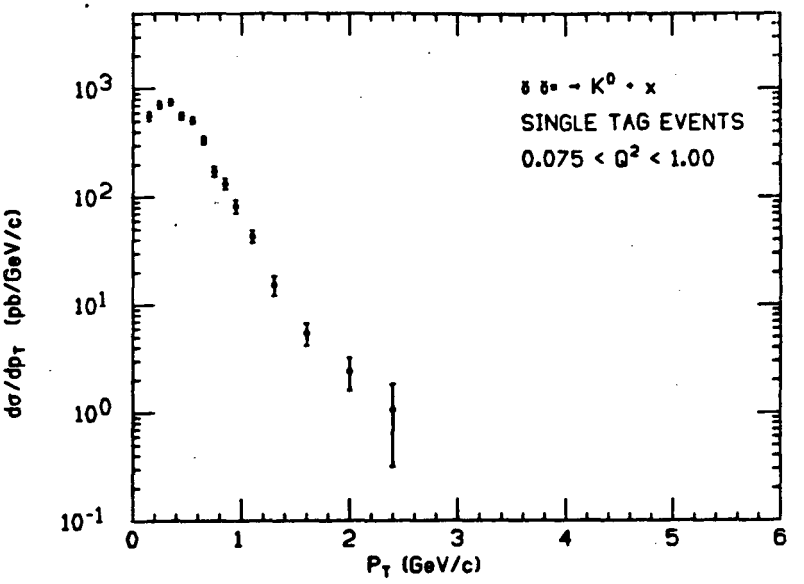

Fig. 10

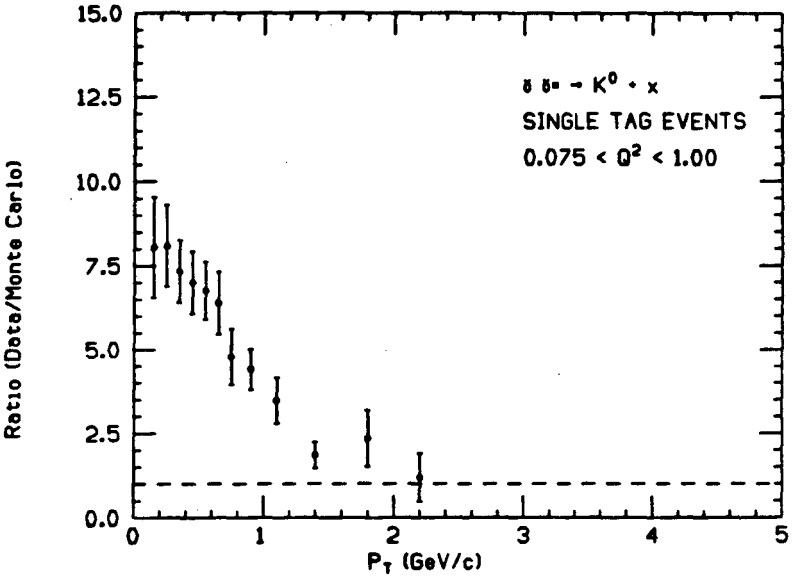

Fig. 11

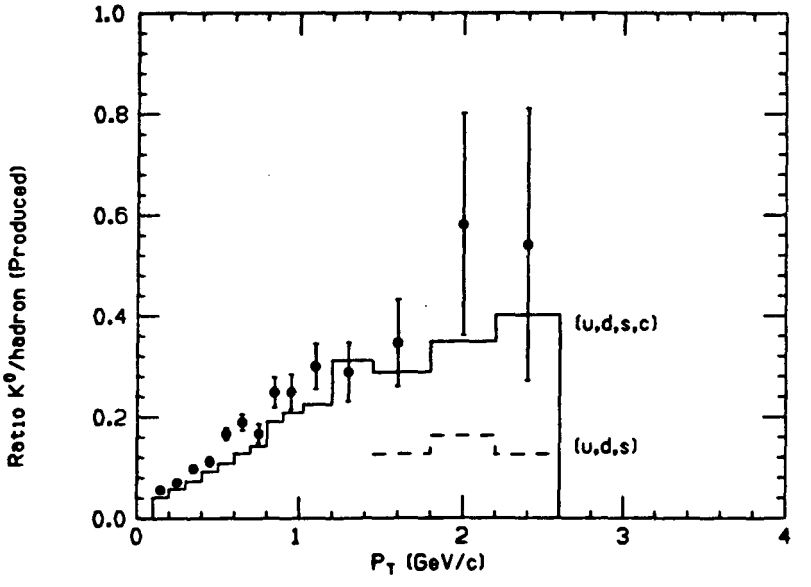

potential error in this comparison:

- p_T smearing; we use p_T with respect to the e^+e^- axis rather than the $\gamma\gamma^*$ axis, and resolution has not been folded into the theory;
- possible "trigger bias" shift in p_T;
- use of the Equivalent Photon Approximation $\ln(\theta_1/\theta_2)$ factor;
- the VDM contribution is suppressed at finite Q^2 relative to the hard scattering part;
- the calculation neglects charm.

In spite of these problems, we get agreement in the p_T region, between 2 and 3 GeV/c, also sampled by TASSO. At larger values of p_T the discrepancy increases.

Since $d\sigma/dp_T^2$ is expected to scale as p_T^{-4} for hard scattering, we show the $p_T^3 d\sigma/dp_T$ distribution in Fig. 7. The flattening of the data above $p_T \simeq 2$ GeV/c confirms this picture. Following PLUTO[5] we define $\tilde{R}$ as the ratio of charged hadrons actually observed to charged hadrons predicted to be observed by the hard scattering Monte Carlo. The p_T distribution of $\tilde{R}$ is shown in Fig. 8. At this point in the analysis we have arbitrarily normalized the Monte Carlo to make $\tilde{R} \simeq 1.0$ at large p_T. We use this normalization for all future comparisons. Again, the flattening near $p_T \simeq 2.0$ confirms the hard scattering picture together with the universality of the LUND fragmentation parameters (tuned in e^+e^- annihilation).

We now turn to the inclusive K^0 production and show the acceptance corrected p_T distribution in Fig. 9. Although the statistics are more limited, we again see evidence of a change in slope between 1.5 and 2.0 GeV/c. If we again calculate $\tilde{R}$ (with the same normalization as in Fig. 8) (see Fig. 10), we again approach unity from above. Comparing Figs. 5 and 9 we notice that while K^0's are only a small part of the total hadrons at small p_T, their fraction steadily increases with p_T. Fig. 11 explicitly shows this fraction as a function of p_T. The solid histogram is the corresponding ratio of produced K^0's to produced charged hadrons in our hard scattering Monte Carlo, including (u,d,s,c) quarks. The dotted curve is the result of the same Monte Carlo with the contribution from charmed quarks omitted. Although the errors are still large, we can see the necessity of including charm. Remember that because it depends on the fourth power of the quark charge, charmed quarks should contribute almost half the cross section above charm threshold. Unfortunately we do not have enough statistics to see convincing evidence of direct charm production (D*'s).

We now turn to the inclusive production of vector mesons. In Fig. 12 we show

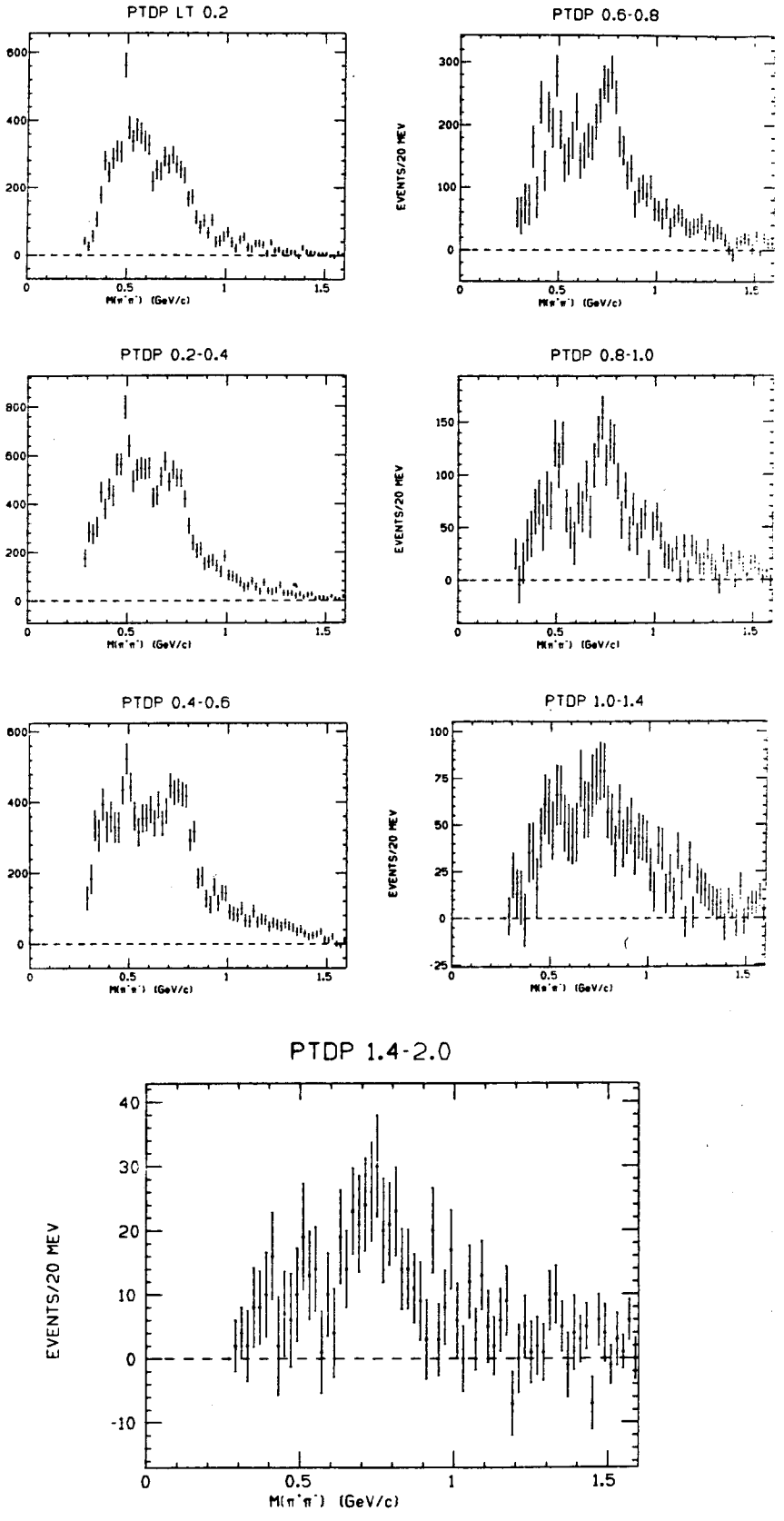
PTDP LT 0.2
PTDP 0.6-0.8
PTDP 0.2-0.4
PTDP 0.8-1.0
PTDP 0.4-0.6
PTDP 1.0-1.4
EVENTS/20 MEV
M(π⁺π⁻) (GeV/c)

PTDP 1.4-2.0
EVENTS/20 MEV
M(π⁺π⁻) (GeV/c)

Fig. 12

Fig. 13

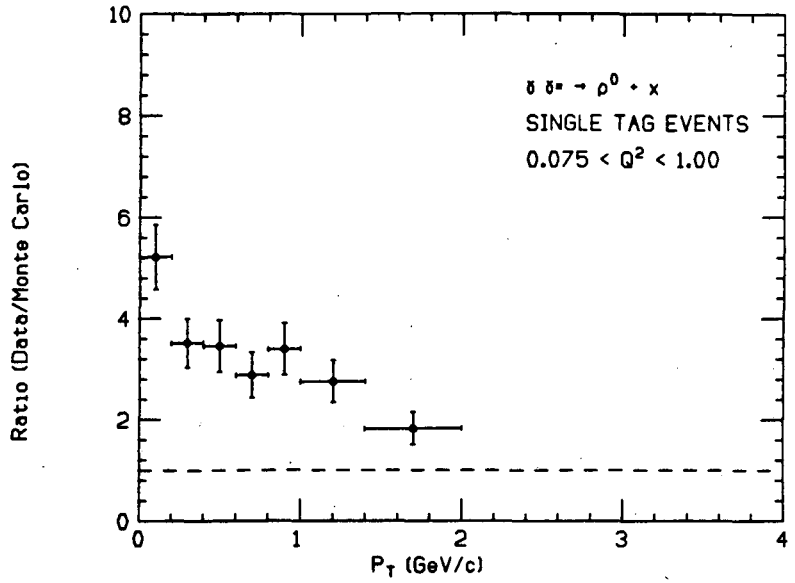

Fig. 14

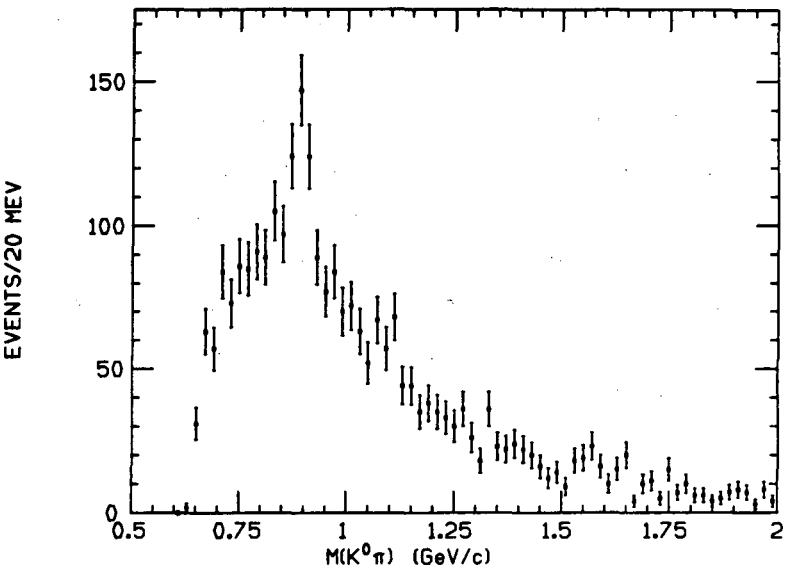

Fig. 15

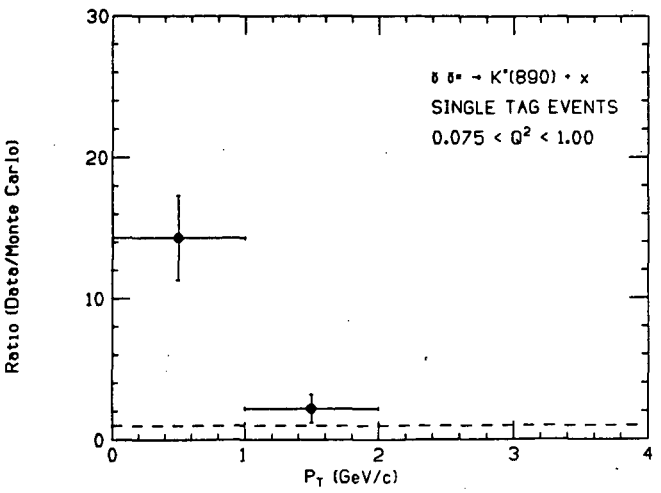

the difference between the number of UNLIKE sign pairs (treated as pions) and that of LIKE sign pairs as a function of $m_{\pi\pi}$, for several intervals of p_T. The like sign distribution is usually a good indicator of the combinatorial background. We see clear K^0 and ρ^0 peaks in every case. The present Monte Carlo lacks the major ρ^0 producing VDM component, but can be used for a first approximation to the ρ^0 detection efficiency. Again we take (see Fig. 13) the ratio of observed ρ^0's in the data and in the Monte Carlo and again see the approach towards unity at the highest p_T. Fig. 14 shows the $K^0\pi^\pm$ mass spectrum and gives clear evidence of K*(890) production. Although the statistics are limited, we can divide the data into two bins; $p_T < 1.0$ GeV/c and $p_T > 1.0$ GeV/c. The K*(890) peak appears in both intervals, and again the ratio, $\tilde{R}$, of observed events to Monte Carlo approaches unity from above (Fig. 15).

There have been several recent reviews of the GGLP effect,[6] but I remind you of two such results in Fig. 16: that of our own SPEAR data at the ψ and the recent TASSO e^+e^- annihilation data. Here the ratio of LIKE to UNLIKE pairs R_U^L is plotted against the variable $Q^2 \equiv m_{\pi\pi}^2 - 4m_\pi^2$. In Fig. 17 we then show this ratio, for all the $\gamma\gamma$ data and, to remove the contribution from the $\rho^0\rho^0$ final state, for events with NCHRG ≥ 5. Thus we have now observed the GGLP effect for $\gamma\gamma^*$ interactions, too. A fit to the form $R_U^L(Q^2) = \gamma(1 + \alpha e^{-r^2Q^2})$ gives $\gamma = 1.04 \pm 0.02$, $\alpha = 0.93 \pm 0.08$ and r (the effective radius of the pion source distribution) $= 0.79 \pm 0.10$ fermi.

II. CHARGED MESON PAIR PRODUCTION

In a QCD model, Brodsky and Lepage[7] have made the absolute predictions shown in Fig. 18. For charged pion pairs these predictions are rather insensitive to assumptions concerning the contributing amplitudes. We indicate the region of cos θ^* accessible to the Mark II detector. Untagged two prong events with $m_{\pi\pi} > 1.7$ GeV, with visible energy $< 0.4\ E_{CM}$, and with net $p_T < 300$ MeV/c are first selected. A brute force application of the liquid argon and muon detectors is then used to reduce the contribution of the dominant eeee and ee$\mu\mu$ final states to an acceptable level.[8]

Since we do not distinguish kaons from pions, Monte Carlo detection efficiencies are determined for each type of particle. The ansatz of reference (7) that

Fig. 16

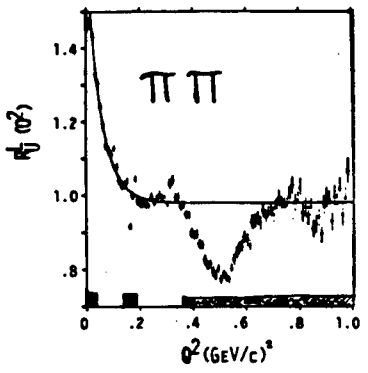
ππ
1.4
1.2
1.0
.8
0
.2
.4
.6
.8
1.0
Q² (GeV/c)²

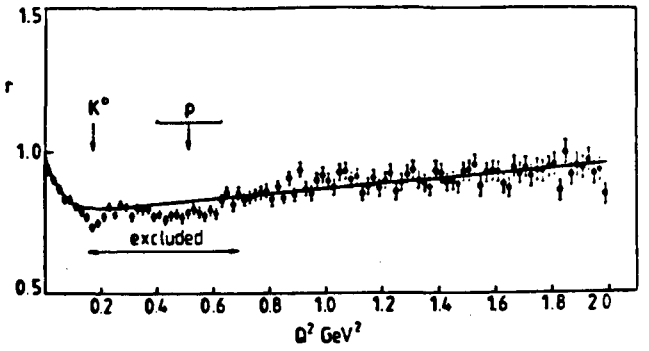
1.5
1.0
0.5
r
K°
ρ
excluded
0.2
0.4
0.6
0.8
1.0
1.2
1.4
1.6
1.8
2.0
Q² GeV²

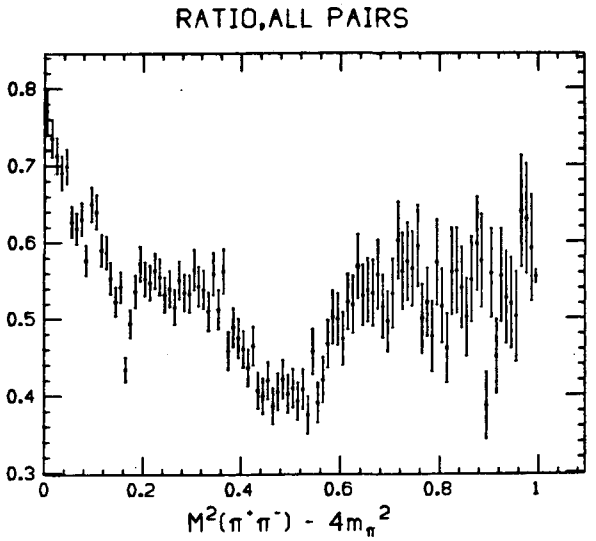
RATIO,ALL PAIRS
0.8
0.7
0.6
0.5
0.4
0.3
0
0.2
0.4
0.6
0.8
1
M²(π⁺π⁻) - 4mπ²

Fig. 17

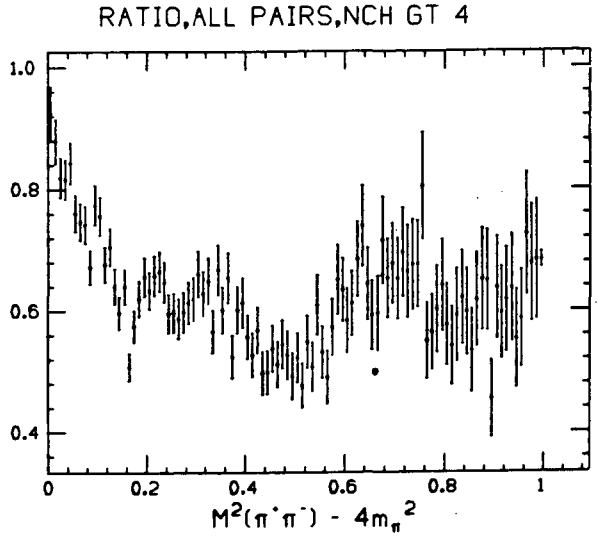
RATIO,ALL PAIRS,NCH GT 4
1.0
0.8
0.6
0.4
0
0.2
0.4
0.6
0.8
1
M²(π⁺π⁻) - 4mπ²

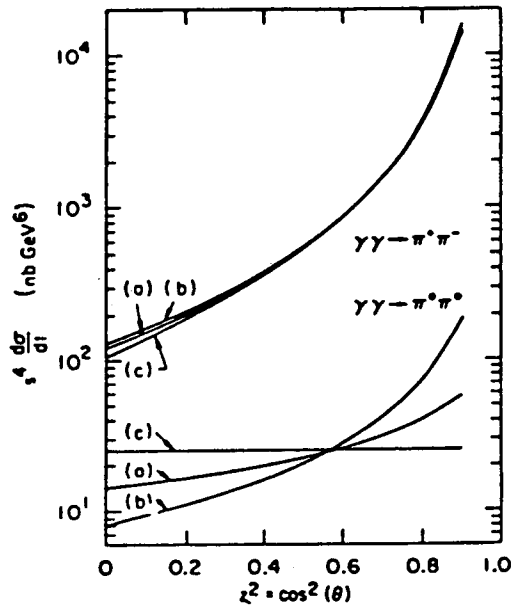

Fig. 18

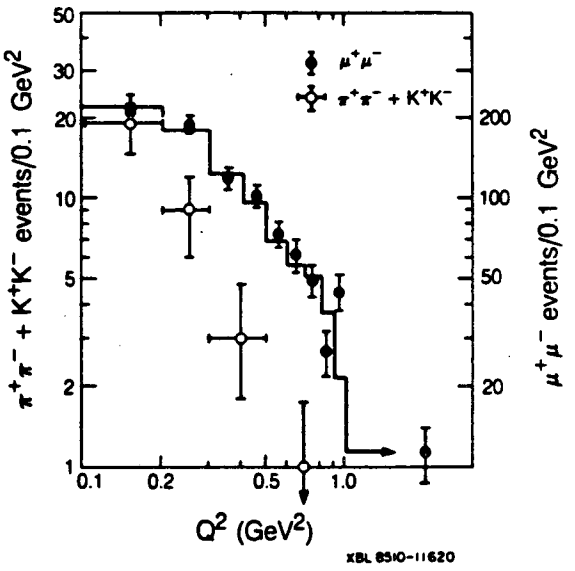

Fig. 21

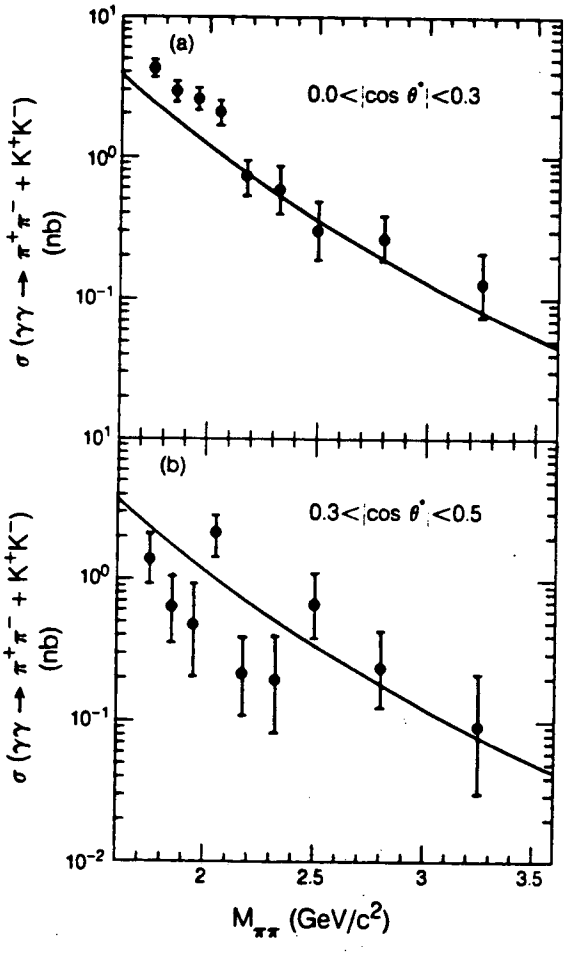

Fig. 19

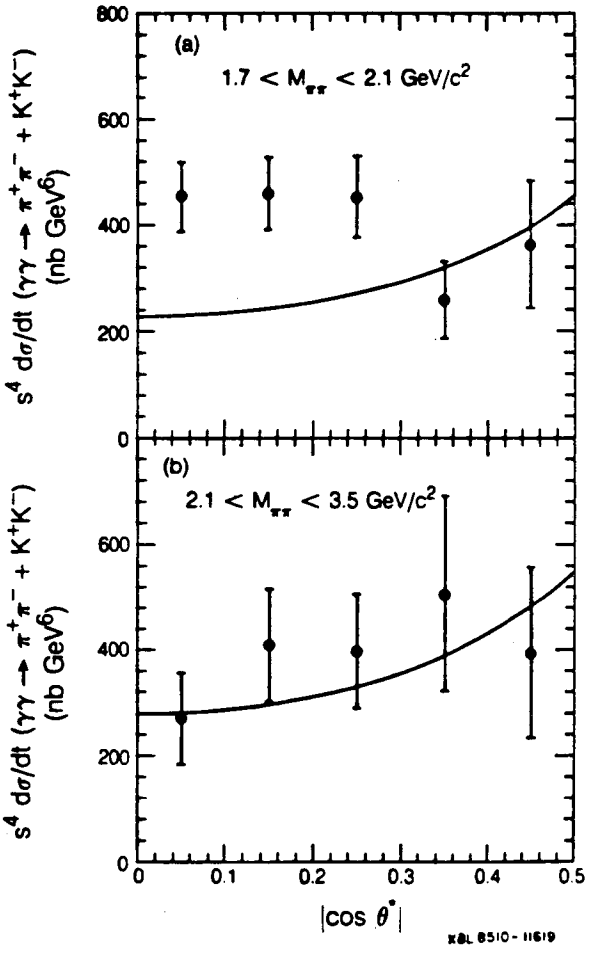

Fig. 20

$\frac{d\sigma}{dt}(\gamma\gamma \to K^+K^-) = 2\,\frac{d\sigma}{dt}(\gamma\gamma \to \pi^+\pi^-)$ is then used with these efficiencies to determine the cross section, $\sigma(\gamma\gamma \to \pi^+\pi^- + K^+K^-)$. Figure 19 shows these results compared to the hard scattering predictions of reference (7). While there is good agreement above 2.1 GeV, there is a discrepancy at the lower masses, where we are presumably still in the resonance region. The PEP 4/9 group has recently separately confirmed[9] these results for $\gamma\gamma \to \pi^+\pi^-$ and $\gamma\gamma \to K^+K^-$. In Fig. 20 we replot this same data as the scaling function $s^4\, d\sigma/dt$ as a function of $|\cos\theta^*|$. The limited statistics and angular range prevent us from checking the predicted rise with $|\cos\theta^*|$ in the mass region above 2.1 GeV. The lower mass region again presumably shows the effect of resonances.

We have also looked at the Q^2 dependence of single tagged events. Almost all these tagged events have $m_{\pi\pi}$ below 2 GeV. The uncorrected experimental Q^2 distribution is shown in Fig. 21 together with the corresponding result for muon pairs. The pion pairs clearly fall off more steeply with Q^2, probably confirming that they are still in the resonance region.

We conclude that even at the relatively modest invariant masses between 2.1 and 3.5 GeV, the predictions of reference (7) are consistent with our observations.[8] Recent calculations[10] indicate that such hard scattering predictions are appropriate at a few GeV.

III. RADIATIVE WIDTH OF THE f′(1525)

The TASSO group has made a very nice measurement[11] of $\Gamma(f' \to \gamma\gamma)$, simultaneously demonstrating the effects of (f, A_2, f') interference in the $K\bar{K}$ final states. Taking advantage of the improved K^0_S identification and measurement made possible by the Mark II vertex detector, we have studied the reaction $\gamma\gamma \to K^0_S\bar{K}^0_S$.

At least one K^0_S is required to be identified as a secondary vertex in four prong events having no additional detected neutrals. The previously discussed cuts in $c\tau$ and decay $\pi^+\pi^-$ mass insure a rather pure sample of events with either one or two secondary K^0's. In Fig. 22 we show the mass of the tracks opposite the identified K^0 in the events with one secondary K^0. The K^0 peak corresponds to decays close to the primary vertex and so an additional mass cut is made as shown. In Fig. 23 we then show the p_T distribution of the remaining events compared to the results of a Monte

Fig. 22

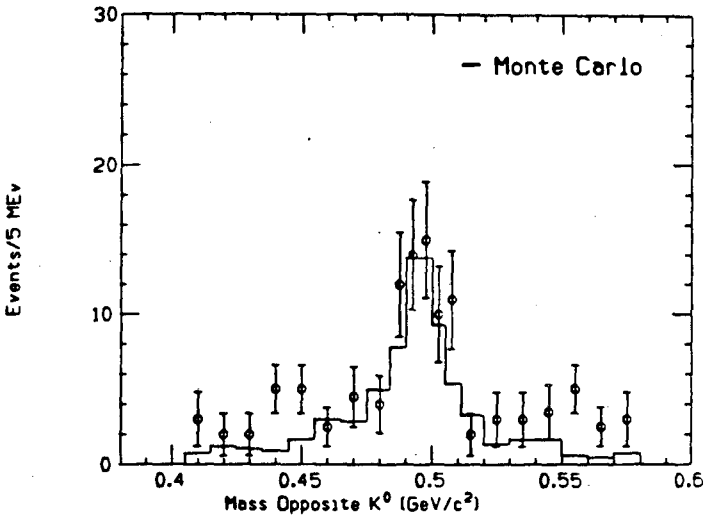

Fig. 23

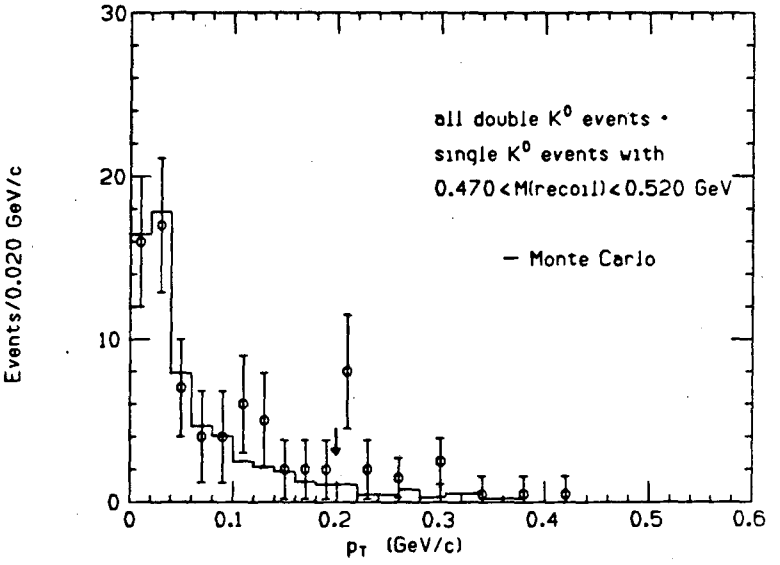

Fig. 24

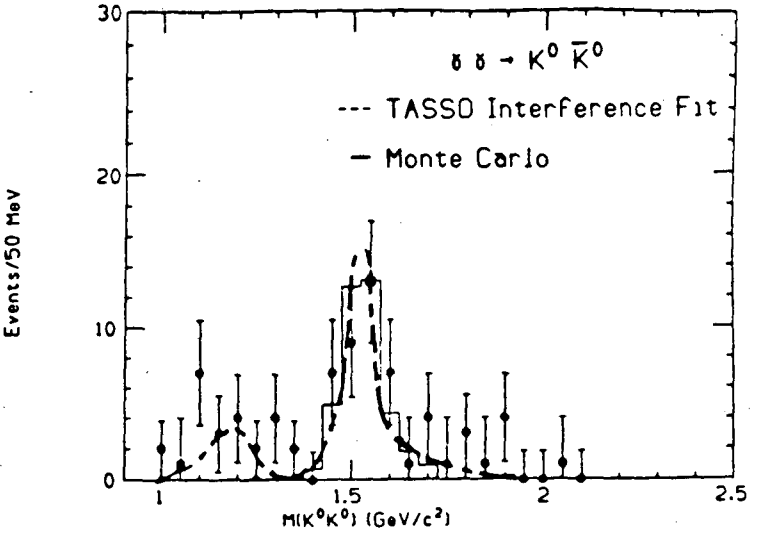

Carlo simulation of $e^+e^- \to e^+e^-f'$. The cut shown defines the final sample whose $K_S^0\overline{K}_S^0$ invariant mass distribution is shown in Fig. 24. The detector acceptance is fairly uniform over this mass plot. The solid histogram is the Monte Carlo prediction for a Breit Wigner f' shape with canonical mass and width, while the dotted curve is the result of the TASSO interference fit[11] with no resolution smearing. From the events in the $f'(1525)$ region we can extract a preliminary result of

$$\Gamma(f' \to \gamma\gamma)\cdot B(f' \to K\overline{K}) = 0.10 \pm 0.04 \text{ KeV}$$

in excellent agreement with the TASSO result.

We acknowledge helpful conversations with S. Brodsky, M. Fontannaz and D. Schiff.

REFERENCES

(1) R. Schindler et al., Phys. Rev. **D24,** 78 (1981).

(2) B. Andersson, G. Gustafson, G. Ingelman, T. Sjostrand, Physics Reports **97,** 31 (1983).

(3) P. Aurenche, A. Douiri, R. Baier, M. Fontannaz, D. Schiff, Z. Phys. **C29,** 423 (1985).

(4) R. Brandelik et al., Phys. Lett. **107B,** 290 (1981).
H. Kolanowski, private communication and BONN-HE-85-34, November 1985.

(5) Ch. Berger et al., Z. Phys. **C26,** 191 (1984).

(6) G. Goldhaber, LESIP I, Bad Honnef, Germany, World Scientific Pub. Co., p. 115 (1984). G. Goldhaber and I. Juricic (LBL-21531), April 1986.

(7) S.J. Brodsky and G.P. Lepage, Phys. Rev. **D30,** 851 (1984).

(8) J. Boyer et al., Phys. Rev. Lett. **56,** 207 (1986).

(9) M. Ronan, presented to this conference.

(10) O.C. Jacob and L.S. Kisslinger, Phys. Rev. Lett. **56,** 225 (1986).

(11) M. Althoff et al., Phys. Lett. **121B,** 216 (1982).
M. Althoff et al., Z. Phys. **C29,** 189 (1985).

LAWRENCE BERKELEY LABORATORY
TECHNICAL INFORMATION DEPARTMENT
UNIVERSITY OF CALIFORNIA
BERKELEY, CALIFORNIA 94720